



**Acoustics'08
Paris**
June 29-July 4, 2008

www.acoustics08-paris.org

New theoretical models for lipid-shelled ultrasound contrast agents

Alexander Doinikov^a, Jill Haac^b and Paul A. Dayton^b

^aBelarus State University, 11 Bobruiskaya Street, 220030 Minsk, Belarus

^bUNC-NCSU Joint Department of Biomedical Engineering, 302 Taylor Hall, CB 7575, Chapel Hill, NC 27599, USA
doinikov@bsu.by

A general theoretical approach to the development of zero-thickness shell models for contrast agent microbubbles, which allows the testing of different rheological laws for encapsulation, is proposed. Based on available experimental data, analysis of the rheological behavior of a lipid shell is made. The problems of existing shell models, such as the dependence of shell parameters on the initial bubble radius and the “compression-only” behavior, are discussed and new theoretical models for their simulation are offered. In particular, it is shown that the inclusion of nonlinear shell viscosity allows one to model the “compression-only” behavior. It is also very important to select an appropriate rheological law describing the dependence of the shell viscosity on the shear rate. A correct choice can reduce considerably the spread of the experimentally estimated values of the shell parameters and eliminate their unnatural dependence on the initial bubble radius.

1 Introduction

Encapsulated gas microbubbles are used in ultrasound medical applications as contrast agents to enhance the acoustic contrast between blood and surrounding tissues and thereby to improve the quality of ultrasonic images. The function of encapsulation is to stabilize microbubbles against fast dissolution and coalescence. Currently available contrast agents are enclosed in a shell of albumin, polymer, or lipid. The present study focuses on lipid-shelled microbubbles.

Proper theoretical description of the rheological behavior of the shell material is of primary importance as it is the shell that determines many of the functional properties of contrast agent microbubbles. Much work has been done on modeling the dynamics of encapsulated microbubbles in an ultrasound field [1-5]. However, existing shell models cannot explain recent experimental observations, such as “compression-only” behavior and the dependence of shell parameters on the initial bubble radius.

The “compression-only” behavior of phospholipid-coated bubbles was discovered by de Jong *et al.* [6]. In the course of an optical ultra high-speed contrast imaging study on individual SonoVue and BR-14 microbubbles, they observed that in some cases the microbubbles only compressed and hardly expanded beyond their initial diameters. Pertinent numerical simulations were carried out using the shell model of de Jong *et al.* [1]. By comparing the experimental data with the simulations, it was concluded that a more sophisticated shell model is required to explain the effect of “compression-only” behavior.

The findings that the shell viscosity of phospholipid-coated microbubbles increases with the initial bubble radius were reported by Morgan *et al.* [3] and more recently by van der Meer *et al.* [7]. Chetty *et al.* [8] report that the shell elasticity seems to behave similarly. In the present paper, we confirm these findings by means of our own experimental data. The result that the shell parameters are found to be highly dependent on the initial bubble radius is of particular interest as it discloses that the current shell models meet with difficulties of fundamental nature. It is clear that physical constants of a material must be independent of the amount of the material. Therefore it is appropriate to suggest that in actual fact the said behavior of the shell viscosity and elasticity is an artifact that arises from an inadequate description of the rheological nature of the encapsulating coating.

The purpose of the present study is to develop new theoretical models that are able to account for the observed experimental effects.

2 Zero-thickness shell model

We begin with the derivation of a general equation for the radial dynamics of a thin-shelled microbubble that provides a way of testing different rheological laws for encapsulation. The most theoretically justified equation of the radial dynamics of an encapsulated bubble is Church’s equation [2]. It can be written as follows

$$R_1 \ddot{R}_1 \left[1 + \beta \frac{R_1}{R_2} \right] + \frac{3}{2} \dot{R}_1^2 \left[1 + \beta \left(\frac{4R_2^3 - R_1^3}{3R_2^3} \right) \frac{R_1}{R_2} \right] = \frac{1}{\rho_S} \left[P_{g0} \left(\frac{R_{10}}{R_1} \right)^{3\gamma} - \frac{2\sigma_1}{R_1} - \frac{2\sigma_2}{R_2} - 4\eta_L \frac{R_1^2 \dot{R}_1}{R_2^3} - P_0 - P_{ac}(t) - S \right], \quad (1)$$

where $R_1(t)$ and $R_2(t)$ are the inner and the outer radii of the encapsulating shell, the overdot denotes the time derivative, $\beta = \rho_L / \rho_S - 1$, ρ_L and ρ_S are the equilibrium densities of the surrounding liquid and the shell, P_{g0} is the equilibrium gas pressure within the bubble, γ is the ratio of specific heats of the gas, R_{10} and R_{20} are the inner and the outer radii of the shell at rest, σ_1 and σ_2 are the surface tension coefficients for the gas-shell and the shell-liquid interfaces, η_L is the shear viscosity of the liquid, P_0 is the hydrostatic pressure in the liquid, and $P_{ac}(t)$ is the driving acoustic pressure. The effect of encapsulation is described by the term S which is given by

$$S = -3 \int_{R_1}^{R_2} \frac{\tau_{rr}(r, t)}{r} dr, \quad (2)$$

where r is the radial coordinate of a spherical coordinate system with the origin at the center of the bubble, and $\tau_{rr}(r, t)$ is the radial component of the stress deviator of the shell.

Equation (1) is valid for bubbles with a shell of finite thickness. However, most types of contrast agents have very thin shells. This is especially true for lipid-coated bubbles. For such bubbles, Eq. (1) is redundant from the numerical point of view, and going to the limit of thin shell is worthwhile. In the limit of thin shell, Eq. (1) reduces to

$$R\ddot{R} + \frac{3}{2}\dot{R}^2 = \frac{1}{\rho_L} \left[P_{g0} \left(\frac{R_0}{R} \right)^{3\gamma} - \frac{2\sigma}{R} - 4\eta_L \frac{\dot{R}}{R} - P_0 - P_{ac}(t) - S \right], \quad (3)$$

where $R(t)$ denotes the radius of the gas-liquid interface, $R_0 = R(0)$, and σ is the surface tension at the gas-liquid interface. In the same limit, the term S becomes

$$S = -\frac{3\varepsilon}{R} \tau_{rr}(r, t) \Big|_{r=R} \quad (4)$$

with ε denoting the shell thickness. Substituting different expressions for τ_{rr} into Eq. (4), one can apply different rheological laws to the bubble shell. This equation shows how existing constitutive equations for the stress tensor τ_{ij} , which are normally specified in the *bulk* form, can be correctly recast to a *surface* form required in Eq. (3).

3 Rheology of lipid encapsulation

The purpose of this section is to explain why existing shell models cause the shell parameters to be dependent on the initial bubble radius. By way of example let us consider the widely used shell model proposed by de Jong *et al.* [1]. It can be represented as [7]

$$S = 4\kappa_S \dot{R}/R^2 + 4\chi(1/R_0 - 1/R), \quad (5)$$

where κ_S is the shell surface viscosity and χ is the shell surface elasticity. In a qualitative sense, the de Jong model is identical to the Church model [2, 5], based on the Kelvin-Voigt constitutive equation, and the Sarkar model [4].

To evaluate the shell parameters appearing in Eq. (5), experimental radius-time curves for twenty microbubbles of various radii were used. The curves were acquired for a home-made phospholipid-coated contrast agent similar to Definity® [9], insonified with a 20-cycle, 3.0 MHz, 100 kPa acoustic pulse. The shell parameters were evaluated by fitting simulated radius-time curves to the experimental data by the least squares method. The best-fit values of κ_S and χ versus the initial bubble radius are shown by circles in Figs. 1(a) and 1(b), respectively. Each circle represents the best fit for one experimental curve. The solid lines show the linear regression for the best-fit values. It is seen that both the shell viscosity and the shell elasticity demonstrate a conspicuous increase with the initial bubble radius.

Van der Meer *et al.* [7] hypothesized that in reality the observed dependence of the shell viscosity on the initial bubble radius is a consequence of the fact that the shell viscosity is dependent on the shear rate, which is proportional to \dot{R}/R in our case. Figure 2(a) confirms this hypothesis. It shows the dependence between the shell viscosity and the maximum shear rate for the experimental data considered. The shell viscosity was evaluated by the de Jong model, as in Fig. 1(a), and the maximum shear rate, which is estimated as the maximum value of \dot{R}/R , was calculated directly from the experimental radius-time curves. One can see that the shell viscosity decreases as the

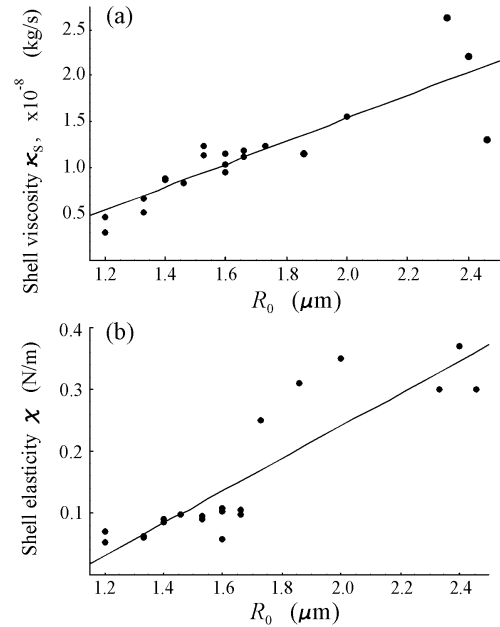


Fig.1 Best-fit values of the shell viscosity and elasticity versus the initial bubble radius for the de Jong model.

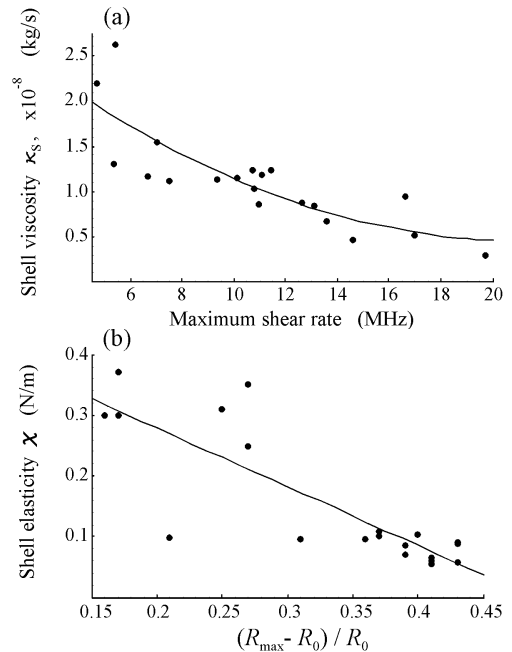


Fig.2 (a) Shell viscosity versus maximum shear rate. (b) Shell elasticity versus deformation strength.

shear rate increases. This type of rheological behavior is known as *shear thinning*. Thus Fig. 2(a) suggests that the lipid coating is a shear-thinning material and hence the observed dependence of κ_S on R_0 is seeming. It arises because the de Jong model does not take into account the real rheological nature of the shell viscosity.

A more physical picture of the behavior of the shell elasticity can be obtained by plotting χ as a function of deformation strength. As a measure of the deformation strength, the quantity $(R_{\max} - R_0)/R_0$ can be taken. The plot of χ versus the estimated deformation strength is shown in Fig. 2(b). The values of χ were evaluated by the de Jong model, as in Fig. 1(b), and the quantity $(R_{\max} - R_0)/R_0$ was calculated directly from the experimental radius-time curves. Figure 2(b) reveals that

the shell elasticity decreases as the deformation strength increases. This rheological effect is known as *strain softening*. Thus there is reason to believe that the lipid coating has the properties of both shear-thinning and strain-softening material. Therefore the theory for the shell elasticity should be revised as well.

In currently existing shell models, the viscous and the elastic shell terms have the simplest possible form, namely, the linear form. This linear theory assumes that the viscous and the elastic stresses acting inside the lipid shell are proportional to the shell shear rate and the shell strain, respectively, with constant coefficients of proportionality κ_S and χ . The analysis presented here shows that a more general, nonlinear theory for both the viscous and the elastic shell terms is required. In what follows, the nonlinear theory for viscous stress will be considered. Theory for elastic stress will be given elsewhere.

4 Nonlinear viscosity

4.1 General theory

In the general case, the relationship between the viscous stress tensor and the rate-of-strain tensor is written as [10]

$$\tau_{ij}^{(vis)} = F(v_{ij}), \quad (6)$$

where $\tau_{ij}^{(vis)}$ is the viscous stress tensor, F is an arbitrary function, and v_{ij} is the rate-of-strain tensor. Actually, the viscous stress tensor can be also dependent on other kinematic quantities in addition to the rate-of-strain tensor, such as the deformation acceleration. However, if we want to adhere to simple models as far as possible, Eq. (6) should be considered as a next step as compared to the linear viscous term in Eq. (5). In the mathematical basis of rheology [10], it is proven that, according to the so-called principle of material objectivity, if the material is isotropic and incompressible, Eq. (6) must be of the following form:

$$\tau_{ij}^{(vis)} = 2\eta_1(I_2, I_3) v_{ij} + 4\eta_2(I_2, I_3) v_{ik} v_{kj}, \quad (7)$$

where summation over double indices is implied, and η_1 and η_2 are arbitrary functions of the second and the third invariants of v_{ij} . I_2 and I_3 can be specified as

$$I_2 = v_{ik} v_{ki}, \quad I_3 = v_{ik} v_{kj} v_{ji}. \quad (8)$$

For an encapsulated bubble, in view of spherical symmetry, Eq. (7) takes the form

$$\tau_{rr}^{(vis)} = 2\eta_1(I_2, I_3) v_{rr} + 4\eta_2(I_2, I_3) (v_{rr})^2, \quad (9)$$

with

$$v_{rr} = -\frac{2R^2 \dot{R}}{r^3}, \quad I_2 = \frac{6R^4 \dot{R}^2}{r^6}, \quad I_3 = -\frac{2R^6 \dot{R}^3}{r^9} \quad (10)$$

Here, it has been used that $v_{rr} = \partial v / \partial r$, where $v(r, t)$ is the radial component of the particle velocity inside the shell, given by $v = R^2 \dot{R} r^{-2}$ [2, 5].

Let us now assume that the total stress tensor $\tau_{rr}(r, t)$ is given by an equation similar to the Kelvin-Voigt constitutive equation but with a viscous part specified by Eq. (9), i.e.,

$$\tau_{rr} = \tau_{rr}^{(vis)} + 2\mu_S \partial u / \partial r, \quad (11)$$

where μ_S is the bulk shear modulus of the shell and $u(r, t)$ is the radial displacement inside the shell, given by $u = R^2 (R - R_0) r^{-2}$ [2, 5]. Then, using Eqs. (4) and (11), we obtain the term S of Eq. (3) to be

$$S = 4\kappa(\dot{R}/R) \frac{\dot{R}}{R^2} + 4\chi \frac{R_0}{R} \left(\frac{1}{R_0} - \frac{1}{R} \right), \quad (12)$$

where $\chi = 3\epsilon\mu_S$ is the shell surface elasticity and κ is a function of the quantity \dot{R}/R which can be treated as the shell shear rate. Theory cannot indicate a more exact form of the function $\kappa(\dot{R}/R)$ in the case under consideration. The literature on rheology shows that the only way to determine an explicit form of $\kappa(\dot{R}/R)$ is to select a suitable analytical function by using experimental data.

4.2 Modeling of “compression-only” behavior

As mentioned above, it has been found experimentally that many phospholipid-coated contrast agents show “compression-only” behavior, where the microbubbles compress much stronger than expand [6]. The de Jong shell model, Eq. (5), cannot simulate this phenomenon because it predicts the relative ratio of expansion to compression to be close to, or above unity [11]. In [6], it is hypothesized that the “compression-only” behavior may be a result of shell buckling. We will show here that this effect can be modeled in terms of nonlinear shell viscosity. It should be noted that, even if the “compression-only” behavior is really caused by shell buckling, formally mathematically, this effect can be modeled as a change in the shell properties, or, in other words, as a specific behavior of the shell, assuming that the shape of the bubble remains spherical. This way is acceptable because in fact we are interested in the scattered echo from the bubble rather than the radial bubble dynamics per se. Therefore, if we are able to approximate the scattered signal from a buckled bubble as if it were a signal from a spherical bubble with specific shell properties, it makes no difference whether the real bubble, as a source of the signal, is buckled or not.

Let us assume that the function $\kappa(\dot{R}/R)$ in Eq. (12) takes the form

$$\kappa(\dot{R}/R) = \kappa_0 + \kappa_1 \dot{R}/R, \quad (13)$$

where κ_0 and κ_1 are constants. For $\kappa_1 = 0$, Eq. (12) reduces to the Kelvin-Voigt shell model. As an example, Fig. 3 shows two radius-time curves that were calculated by Eqs. (3), (12), and (13) for a bubble with $R_0 = 2.03 \mu\text{m}$, insonified with a 6-cycle, 1.8 MHz, 100 kPa acoustic pulse. These parameters correspond to Fig. 2 in [6]. The curve in

Fig. 3(a) was calculated at $\chi = 0.5$ N/m, $\kappa_0 = 1.5 \times 10^{-8}$ kg/s, and $\kappa_1 = 0$, i.e., that is a curve given by the Kelvin-Voigt shell model. The curve in Fig. 3(b) was calculated for the same parameters except that $\kappa_1 = 1.0 \times 10^{-14}$ kg. One can see that this curve does show a response that is very much similar to the “compression-only” behavior, with sharp edges in the compression phase as reported in [6].

Figure 4 represents results given by the Kelvin-Voigt model and the model with Eq. (13) when a simulated radius-time curve is fitted to one of our experimental radius-time curves showing “compression-only” behavior. An example of the experimental radius-time curve is displayed in Fig. 4(a). The curve was acquired for a phospholipid-coated bubble with $R_0 \approx 1.4$ μm . The bubble was insonified with a 20-cycle, 3.0 MHz, 100 kPa acoustic pulse. Figure 4(b) shows the best fit that was obtained by the least squares method using the Kelvin-Voigt model ($\kappa_1 = 0$). The solid line represents the simulated radius-time curve and circles indicate the experimentally measured points. Figure 4(b) corresponds to the part of the experimental curve in Fig. 4(a) between 3 and 5 μs . The best fit given by the model with Eq. (13) is shown in Fig. 4(c). One can see that the application of Eq. (13) improves considerably agreement between the theoretical curve and the experimental data.

4.3 Modeling of shear-thinning behavior

Equation (13) allows one to model “compression-only” behavior. However, the dependence of κ_0 and κ_1 on the initial bubble radius still persists. This is confirmed by Fig. 5, which presents the best-fit values of κ_0 and κ_1 versus the initial bubble radius for the same experimental data as in Sec. 3. The best-fit values of κ_0 and κ_1 are shown by circles in Figs. 5(a) and 5(b), respectively. The values of χ remain virtually the same as in Fig. 1(b). Note that Fig. 5(a) is almost identical to Fig. 1(a). This means that the presence of the term $\kappa_1 \dot{R}/R$ in Eq. (13) does not virtually change the constant component of the shell viscosity, κ_0 , as compared to the shell viscosity of the de Jong model, κ_S . This is only natural if we take into consideration that the term $\kappa_1 \dot{R}/R$ is responsible for “compression-only” behavior, while κ_0 describes the behavior of lipid as a material. If that is true, the spread of the values of κ_1 in Fig. 5(b) can be explained as follows. It is hypothesized in [6] that “compression-only” behavior is a result of initial shell buckling. In its turn, the degree of initial buckling for a particular bubble is likely to be a result of random factors so that bubbles of the same size can have a different degree of initial buckling. Therefore the disordered (statistical) spread of the values of κ_1 is quite expected. This is not the case, however, for κ_0 , which is assumed to be a constant of lipid as a material, and therefore the dependence of this constant on the initial bubble radius requires a further consideration.

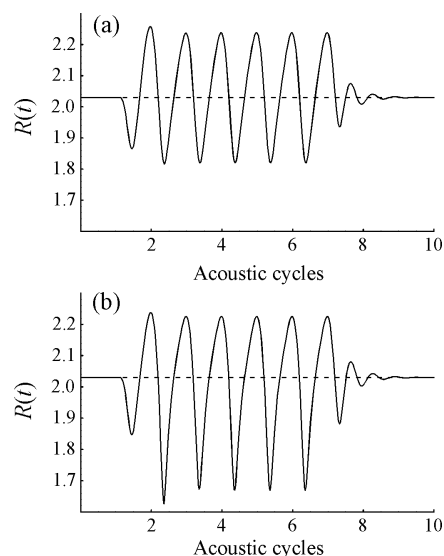


Fig.3 Simulated radius-time curves for a 2.03- μm -radius encapsulated bubble insonified with a 6-cycle, 1.8 MHz, 100 kPa acoustic pulse. (a) The Kelvin-Voigt shell model. (b) The model with the shell viscosity specified by Eq. (13).

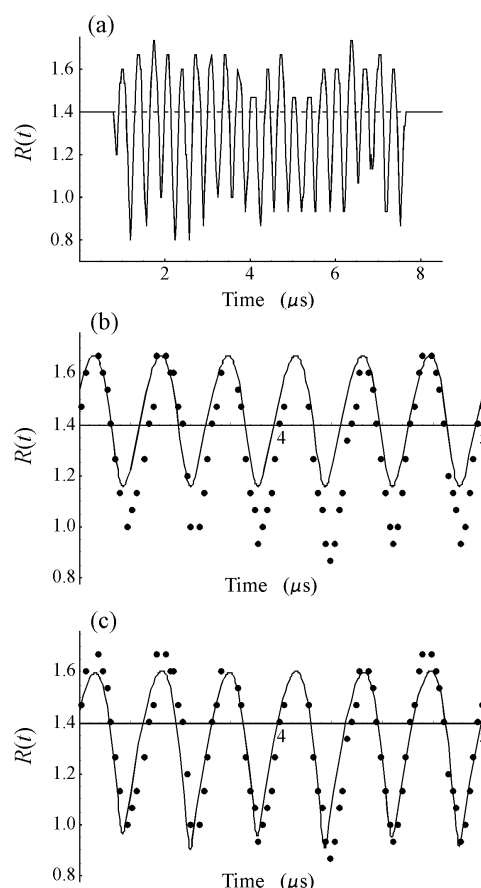


Fig.4 Fitting of an experimental radius-time curve showing “compression-only” behavior. (a) The experimental radius-time curve. (b) The best fit given by the Kelvin-Voigt shell model. (c) The best fit given by the model with the shell viscosity specified by Eq. (13).

Considering Fig. 2(a), we should seek a law for κ_0 that is to describe shear-thinning behavior. There are many laws used in the rheology of polymers to model shear-thinning behavior. Following the way of simple models as before, let us try the following equation:

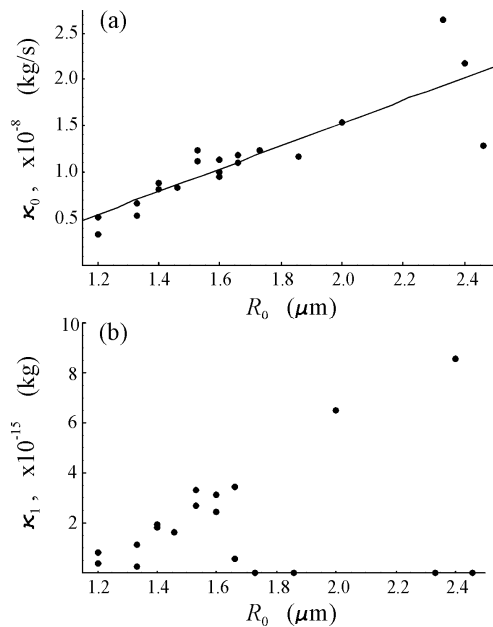


Fig.5 Best-fit values of κ_0 and κ_1 versus the initial bubble radius. Fitting was done by using Eqs. (12) and (13).

$$\kappa(\dot{R}/R) = \kappa_0 \left(1 + \alpha |\dot{R}/R|\right)^{-1} + \kappa_1 \dot{R}/R, \quad (14)$$

The first term in this equation is a particular case of the so-called Cross law. With Eq. (14), setting $\alpha = 4 \mu\text{s}$, the fitting of the same experimental data as in Figs. 1 and 5 gives the values of κ_0 shown in Fig. 6, the values of κ_1 remaining the same as in Fig. 5(b). It is seen that the spread of the values of κ_0 in Fig. 6 is noticeably smaller than in Fig. 5(a), and we now have $(\kappa_0)_{\max}/(\kappa_0)_{\min} \approx 2.4$ instead of $(\kappa_0)_{\max}/(\kappa_0)_{\min} \approx 8$ as in Fig. 5(a).

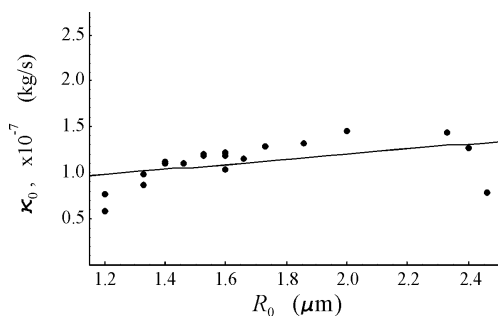


Fig.6 Best-fit values of κ_0 versus the initial bubble radius. Fitting was done by using Eqs. (12) and (14).

5 Conclusion

Using experimental data, it was shown that the lipid coating exhibits the properties of both shear-thinning and strain-softening material. It was proposed to use the nonlinear viscous theory for the modeling of the “compression-only” behavior and the dependence of the shell viscosity on the shear rate. It was shown that the application of a correct rheological law can eliminate the unnatural dependence of the shell viscous coefficient on the initial bubble radius, which is shown by currently existing models.

Acknowledgments

A. A. D. wishes to acknowledge the financial support of the International Science and Technology Center (ISTC) under Contract No. B-1213. P. A. D. is supported by the NIH Roadmap for Medical Research, EB005325. We thank Katherine Ferrara for use of the high-speed imaging system.

References

- [1] N. de Jong, R. Cornet, C. T. Lancée, "Higher harmonics of vibrating gas-filled microspheres. Part one: simulations", *Ultrasonics* 32, 447-453 (1994).
- [2] C. C. Church, "The effect of an elastic solid surface layer on the radial pulsations of gas bubbles", *J. Acoust. Soc. Am.* 97, 1510-1521 (1995).
- [3] K. E. Morgan, J. S. Allen, P. A. Dayton, J. E. Chomas, A. L. Klibanov, K. W. Ferrara, "Experimental and theoretical evaluation of microbubble behavior: Effect of transmitted phase and bubble size", *IEEE Trans. Ultrason. Ferroelect. Freq. Contr.* 47, 1494-1509 (2000).
- [4] K. Sarkar, W. T. Shi, D. Chatterjee, F. Forsberg, "Characterization of ultrasound contrast microbubbles using in vitro experiments and viscous and viscoelastic interface models for encapsulation", *J. Acoust. Soc. Am.* 118, 539-550 (2005).
- [5] A. A. Doinikov, P. A. Dayton, "Spatio-temporal dynamics of an encapsulated gas bubble in an ultrasound field", *J. Acoust. Soc. Am.* 120, 661-669 (2006).
- [6] N. de Jong, M. Emmer, C. T. Chin, A. Bouakaz, F. Mastik, D. Lohse, M. Versluis, "'Compression-only" behavior of phospholipid-coated contrast bubbles", *Ultrasound Med. Biol.* 33, 653-656 (2007).
- [7] S. M. van der Meer, B. Dollet, M. M. Voormolen, C. T. Chin, A. Bouakaz, N. de Jong, M. Versluis, D. Lohse, "Microbubble spectroscopy of ultrasound contrast agents", *J. Acoust. Soc. Am.* 121, 648-656 (2007).
- [8] K. Chetty, C. A. Sennoga, J. V. Hainal, R. J. Eckersley, E. Stride, "High speed optical observations and simulation results of lipid based microbubbles at low insonation pressures", in *Proceedings of the 2006 IEEE International Ultrasonics Symposium* (IEEE, Vancouver, Canada, 2006), pp. 1354-1357.
- [9] S. Zhao, M. A. Borden, S. H. Bloch, D. Kruse, K. W. Ferrara, P. A. Dayton, "Radiation-force assisted targeting facilitates ultrasonic molecular imaging", *Mol. Imaging* 3, 135-148 (2004).
- [10] C. Truesdell, *A First Course in Rational Continuum Mechanics* (The Johns Hopkins University, Baltimore, Maryland, 1972).
- [11] M. Emmer, A. van Wamel, D. E. Goertz, N. de Jong, "The onset of microbubble vibration", *Ultrasound Med. Biol.* 33, 941-949 (2007).